Article

Cell Stem Cell

Sox9 Controls Self-Renewal of Oncogene Targeted Cells and Links Tumor Initiation and Invasion

Graphical Abstract

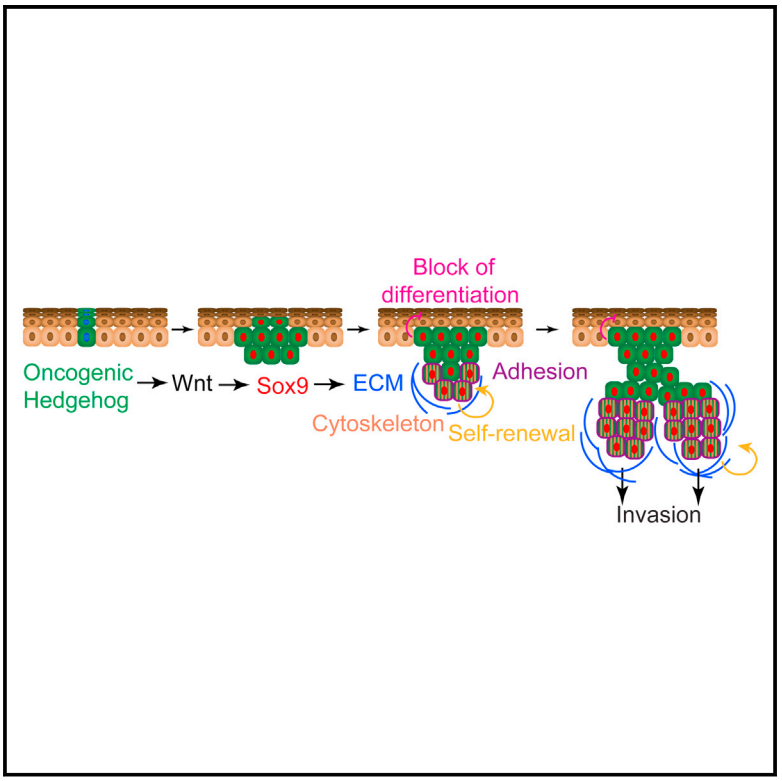

Authors

Jean-Christophe Larsimont, Khalil Kass Youssef, Adriana Sánchez-Danés, ..., Jean-Marie Vanderwinden, Francois Fuks, Cédric Blanpain

Correspondence

cedric.blanpain@ulb.ac.be

In Brief

Using mouse models of BCC, Larsimont et al. show that Sox9 is required for self-renewal of oncogene-expressing cells and BCC formation. Transcriptional profiling combined with ChIP sequencing uncovered a cancer-specific gene network regulated by Sox9 that promotes stemness, represses differentiation, and induces ECM and cytoskeleton remodeling required for tumor invasion.

Highlights

- Sox9 is required for BCC formation in a Wnt/β-catenin-dependent manner
- ChIP-seq and microarray reveal a Sox9-controlled cancer-specific gene network
- Sox9 promotes BCC stemness and self-renewal and inhibits differentiation
- Sox9 controls ECM and cytoskeleton remodeling during tumor invasion

Accession Numbers

GSE68613
GSE68755

Larsimont et al., 2015, Cell Stem Cell *17*, 60–73
July 2, 2015
http://dx.doi.org/10.1016/j.stem.2015.05.008

CellPress

Cell Stem Cell
Article

Sox9 Controls Self-Renewal of Oncogene Targeted Cells and Links Tumor Initiation and Invasion

Jean-Christophe Larsimont,[1] Khalil Kass Youssef,[1] Adriana Sánchez-Danés,[1] Vijayakumar Sukumaran,[1] Matthieu Defrance,[3] Benjamin Delatte,[3] Mélanie Liagre,[1] Pieter Baatsen,[4] Jean-Christophe Marine,[5] Saskia Lippens,[6,7,8] Christopher Guerin,[6,7,8] Véronique Del Marmol,[9] Jean-Marie Vanderwinden,[1] Francois Fuks,[3] and Cédric Blanpain[1,2,*]

[1]Université Libre de Bruxelles, IRIBHM, Brussels 1070, Belgium
[2]WELBIO, Université Libre de Bruxelles, Brussels 1070, Belgium
[3]Laboratory of Cancer Epigenetics, Faculty of Medicine, Université Libre de Bruxelles, Brussels 1070, Belgium
[4]EM-Facility EMoNe, VIB BIO Imaging Core, Center for Human Genetics Katholieke Universiteit Leuven, Leuven 3000, Belgium
[5]Laboratory for Molecular Cancer Biology, Center for the Biology of Disease, VIB, Leuven 3000, Belgium
[6]Inflammation Research Center, Image Core Facility, VIB, Ghent 9052, Belgium
[7]VIB Bio Imaging Core, Ghent 9052, Belgium
[8]Department of Biomedical Molecular Biology, Ghent University, Ghent 9052, Belgium
[9]Department of Dermatology, Erasme Hospital, Université Libre de Bruxelles, Brussels 1070, Belgium
*Correspondence: cedric.blanpain@ulb.ac.be
http://dx.doi.org/10.1016/j.stem.2015.05.008

SUMMARY

Sox9 is a transcription factor expressed in most solid tumors. However, the molecular mechanisms underlying Sox9 function during tumorigenesis remain unclear. Here, using a genetic mouse model of basal cell carcinoma (BCC), the most frequent cancer in humans, we show that Sox9 is expressed from the earliest step of tumor formation in a Wnt/β-catenin-dependent manner. Deletion of *Sox9* together with the constitutive activation of Hedgehog signaling completely prevents BCC formation and leads to a progressive loss of oncogene-expressing cells. Transcriptional profiling of oncogene-expressing cells with *Sox9* deletion, combined with in vivo ChIP sequencing, uncovers a cancer-specific gene network regulated by *Sox9* that promotes stemness, extracellular matrix deposition, and cytoskeleton remodeling while repressing epidermal differentiation. Our study identifies the molecular mechanisms regulated by Sox9 that link tumor initiation and invasion.

INTRODUCTION

During tumor initiation, normal cells targeted by oncogenic mutations undergo a series of molecular changes that promote their renewal, leading to their clonal expansion and the acquisition of invasive properties. Although the mutations leading to tumor formation are relatively well known (Stratton, 2011), the temporality of the molecular changes from the first oncogenic mutations to the development of invasive tumors remains poorly understood. It remains unclear what is the relative importance of the cancer cell of origin, the microenvironment, and the molecular changes downstream of the oncogenic stimuli leading to the rewiring of normal cells into fully tumorigenic cells.

Basal cell carcinoma (BCC) is the most common cancer in humans and affects several million new patients each year across the world (Epstein, 2008). BCC arises from constitutive activation of the Hedgehog (HH) signaling pathway following an activating mutation in Smoothened (*Smo*) receptor or loss of Patched1 (*Ptch1*) function (Epstein, 2008). Using mouse models of BCC that allow the expression of oncogenic *Smo* mutation (SmoM2) in different epidermal compartments, we and others have previously shown that long-lived epidermal stem cells (SCs) residing in the interfollicular epidermis (IFE) are the cells of origin of SmoM2-induced BCC during physiological conditions (Wong and Reiter, 2011; Youssef et al., 2010). By transcriptional profiling of SmoM2-expressing cells during BCC initiation, we and others demonstrated that adult IFE SCs undergo a profound reprogramming into a fate that resembles embryonic hair follicle (HF) progenitors (EHFPs) before progressing into invasive tumors and identified Wnt-/β-catenin signaling as the major driver of this cellular reprogramming (Yang et al., 2008; Youssef et al., 2012). However, the molecular mechanisms downstream of Wnt signaling that control tumor formation remain unclear.

Sox9, a transcription factor (TF) that controls cell fate decision during the development and homeostasis of a broad range of tissues, including the HF SCs (HFSCs) (Kadaja et al., 2014; Nowak et al., 2008; Vidal et al., 2005), is expressed in a wide range of cancers, including BCCs (Vidal et al., 2008). *Sox9* deletion prevents tumorigenesis in prostate and pancreatic mouse cancer models (Kopp et al., 2012; Thomsen et al., 2010), and gain and loss of *Sox9* function in human cancer cell lines suggest that *Sox9* inhibits apoptosis and promotes proliferation, invasion, and metastasis (Cai et al., 2013; Camaj et al., 2014; Wang et al., 2008). However, the molecular mechanisms downstream of Sox9 functions in cancer remain unknown.

Here, using conditional deletion of *Sox9* in mouse models of BCC, we investigated the role and the mechanisms underlying *Sox9* function during tumor formation. We found that *Sox9* is

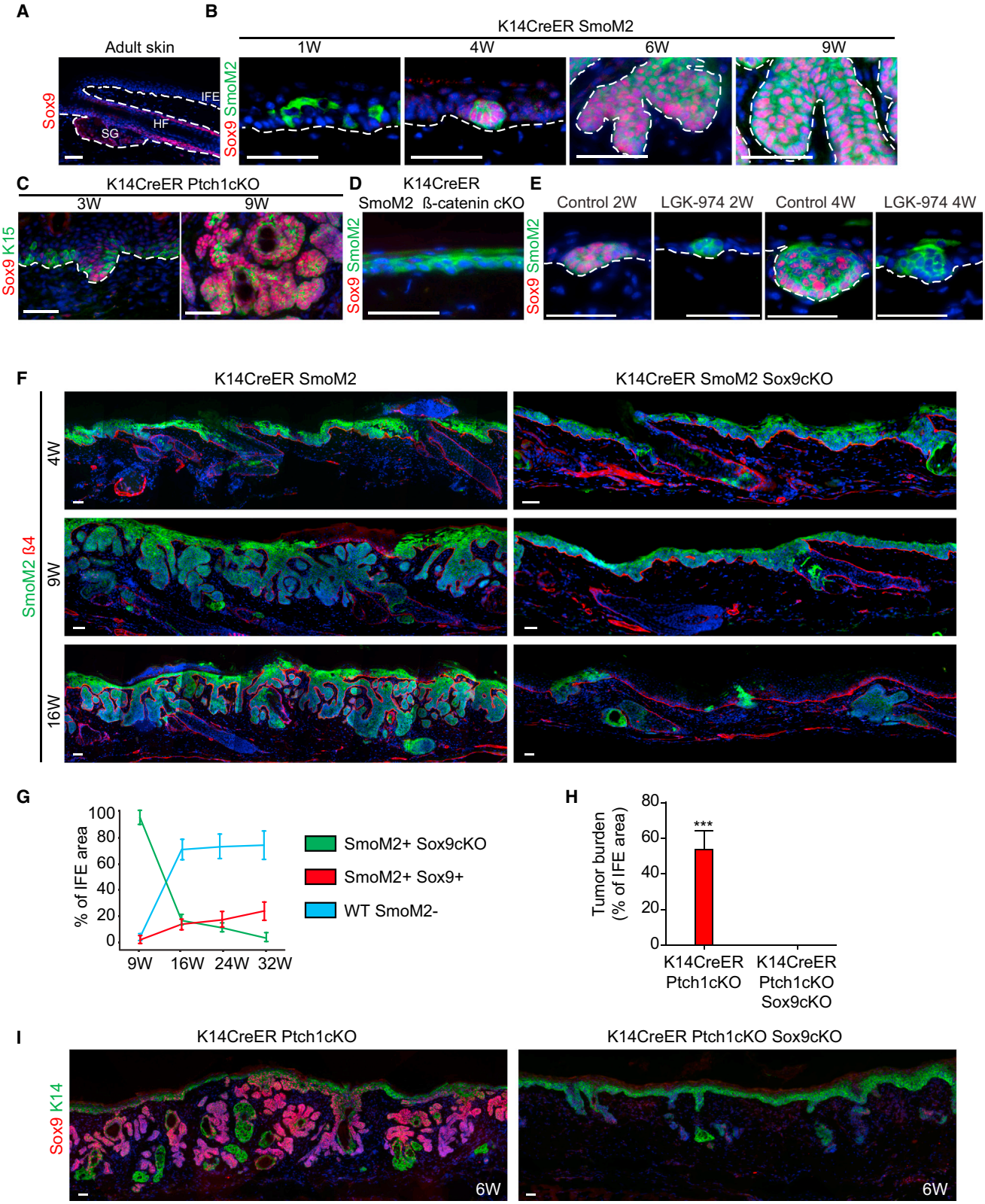

Figure 1. Sox9 Is Required for BCC Initiation and Long-Term Maintenance of Oncogene-Expressing Cells

(A) IF of Sox9 in adult tail skin. SG, sebaceous gland.

(B) IF of Sox9 and SmoM2 in tail epidermis of K14CreER:SmoM2 mice 1, 4, 6, and 9 weeks after TAM administration. Dashed lines represent the BL.

(legend continued on next page)

required downstream of Wnt/β-catenin signaling for the long-term self-renewal of oncogene-expressing cells and tumor formation. Transcriptional profiling combined with chromatin immunoprecipitation (ChIP) sequencing (ChIP-seq) identified a gene-regulatory network (GRN) directly regulated by *Sox9* that controls self-renewing division, differentiation, adhesion, extracellular matrix (ECM), and cytoskeleton remodeling required for the progression of oncogene-targeted cells into invasive tumors.

RESULTS

Sox9 Is Required for the Long-Term Maintenance of Oncogene-Expressing Cells and BCC Formation

To define the role of *Sox9* during tumorigenesis, we first assessed its temporal appearance following oncogenic HH activation in adult epidermal cells. During adult homeostasis, Sox9 is expressed exclusively by HFSCs and their progeny but not by IFE keratinocytes (Figure 1A) (Nowak et al., 2008; Vidal et al., 2005). However, after SmoM2 expression, Sox9 became detectable in the IFE when SmoM2-targeted cells stopped differentiating normally and adopted a placode-like morphology (Figure 1B) and persisted in fully developed BCCs (Figure 1B). Sox9 was also highly expressed in dysplasia and BCC arising from *Ptch1* deletion (Figure 1C), demonstrating that Sox9 expression is a common feature observed during BCC development irrespective of the oncogenic hit. Wnt/β-catenin signaling controls the reprogramming of adult IFE into EHFP-like fate and is required for BCC initiation (Yang et al., 2008; Youssef et al., 2012). To assess whether Wnt/β-catenin signaling is required for the ectopic expression of Sox9 following oncogenic HH signaling, we examined Sox9 expression following concomitant SmoM2 expression and β-catenin deletion. Interestingly, β-catenin deletion completely prevented Sox9 expression following SmoM2 expression 4 weeks following tamoxifen (TAM) administration, a time point at which all SmoM2-expressing dysplasia expressed Sox9 (Figure 1D), suggesting that Wnt/β-catenin signaling is required to initiate Sox9. To substantiate this finding, we assessed whether administration of LGK974, a Wnt signaling inhibitor (Liu et al., 2013), prevents Sox9 expression in SmoM2-induced cells. Oral administration of LGK974 for 14 days, starting 2 weeks after TAM administration, completely prevented Sox9 (Figure 1E), further demonstrating that Wnt signaling is necessary for the initial expression of Sox9 following SmoM2 expression in adult IFE cells. We next assessed whether Wnt signaling is also critical for the maintenance of Sox9 expression. To that end, we induced SmoM2 expression and started treating mice with LGK974 4 weeks after SmoM2 induction, when dysplasia already expressed Sox9 (Figures 1B and S1F). After 2 weeks of LGK974 administration, Sox9 was no longer expressed in SmoM2-expressing cells (Figure 1E), showing that Wnt signaling is required downstream of SmoM2 to initiate and sustain Sox9 expression. Altogether, these data show that oncogenic HH activation in adult IFE leads to Sox9 expression through a Wnt/β-catenin-dependent mechanism.

To determine the role of Sox9 during BCC formation, we performed conditional deletion of *Sox9* together with SmoM2 expression and assessed the impact of *Sox9* deletion on BCC formation (Figures S1A and S1B). Administration of 25 mg TAM over 10 days to K14CreER/Rosa26-SmoM2-YFP/Sox9flox/flox (K14CreER:SmoM2:Sox9cKO) induced SmoM2 expression together with *Sox9* deletion in most IFE cells (>95%) (Figures 1G and S1C). Nine weeks following TAM administration, K14CreER:Rosa26-SmoM2-YFP (K14CreER:SmoM2) mice developed macroscopic hypervascularized lesions in the tail and the ears, while K14CreER:SmoM2:Sox9cKO mice were almost indistinguishable from the wild-type (WT) mice (Figures S1D and S1E). Microscopic examination of the tail epidermis 4 weeks after TAM administration revealed that K14CreER:SmoM2 mice present numerous dysplastic lesions that further progress into BCC 9 weeks after TAM administration (Figure 1F), as previously described (Youssef et al., 2012; Youssef et al., 2010). In sharp contrast, in the absence of Sox9, while SmoM2 was detected in the epidermis of the K14CreER:SmoM2:Sox9cKO, the IFE was hyperplastic or dysplastic but did not present any sign of progression into invasive BCCs (Figure 1F). Surprisingly, 16 weeks after TAM administration, the number of cells expressing SmoM2 dramatically decreased, with a concomitant increase in WT cells (Figures 1F, 1G, and S1G). While covering about 95% of the IFE area 9 weeks after TAM administration, SmoM2+ Sox9cKO cells represented less than 3% of the total IFE cells after 32 weeks (Figures 1F and 1G). These data demonstrate that Sox9 is required for the long-term maintenance of oncogene-expressing cells.

Because it has been shown that BCC arising from Ptch1 loss of function and Gli2 overexpression arise from the HFSCs and their progeny (Grachtchouk et al., 2011; Kasper et al., 2011; Wang et al., 2011), we next determined whether Sox9 is required for BCC formation following *Ptch1* deletion, the most frequent mutation in BCC (Epstein, 2008). While the K14CreER:Ptch1flox/flox (K14CreER:Ptch1cKO) developed numerous BCCs in the ventral skin epidermis 6 weeks following TAM administration, *Sox9* deletion prevented *Ptch1*-induced BCC (Figures 1H and 1I), demonstrating that Sox9 is required for BCC formation regardless of the oncogenic stimuli, the cell of origin, and the body location from where the tumors arise.

(C) IF of Sox9 and K15 in ventral skin in K14CreER:Ptch1cKO mice, showing Sox9 expression at 3 and 9 weeks after TAM administration.
(D) IF of Sox9 in K14CreER:SmoM2:β-catenincKO mice.
(E) IF of Sox9 and SmoM2 in K14CreER:SmoM2 mice treated during 2 weeks with LGK974 or vehicle, starting either 2 or 4 weeks after TAM administration.
(F) IF of SmoM2 and β4 in K14CreER:SmoM2 and K14CreER:SmoM2:Sox9cKO at 4, 9, and 16 weeks after TAM administration.
(G) Quantification of chimerism of SmoM2+ cells deleted for Sox9 cells, WT cells, and SmoM2-expressing cells that escaped *Sox9* deletion at 9, 16, 24, and 32 weeks after TAM administration to K14CreER:Rosa-SmoM2:Sox9cKO mice (9 weeks, n = 3; 16 weeks, n = 6; 24 weeks, n = 4; 32 weeks, n = 3 mice).
(H) Quantification of the tumor burden in K14CreER:Ptch1cKO and K14CreER:Ptch1cKO:Sox9cKO mice (n = 3 mice in each group) 6 weeks following TAM administration.
(I) IF of Sox9 and the basal marker K14 in ventral skin of K14CreER:Ptch1cKO and K14CreERPtch1Sox9cKO mice.
Data represent the mean and SEM of at least three biological replicates. *$p \leq 0.05$; **$p \leq 0.01$; ***$p \leq 0.001$. The scale bars represent 50 μm.

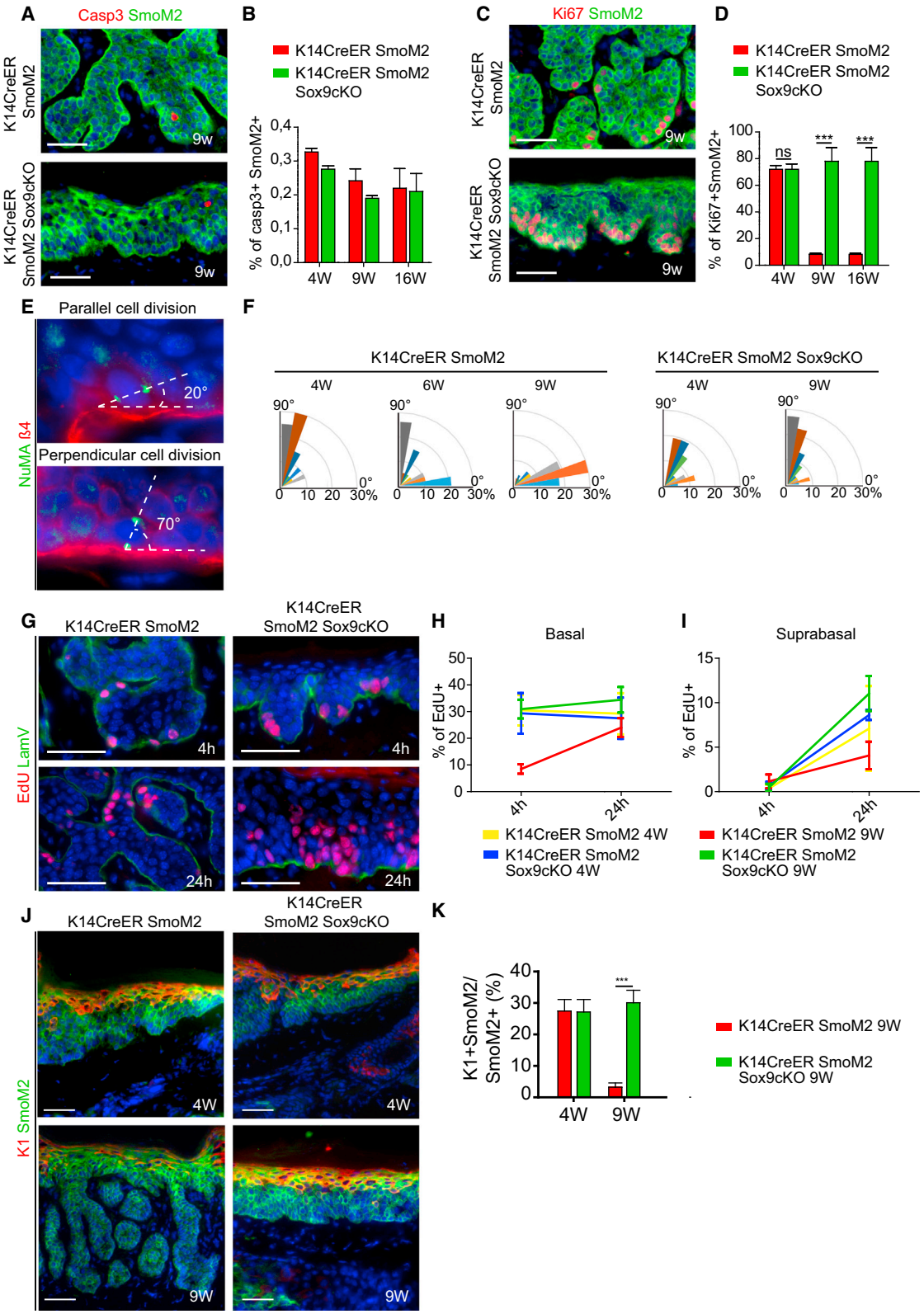

Figure 2. Sox9 Promotes Symmetric Renewal of Oncogene-Expressing Cells

(A) IF of activated caspase-3 and SmoM2 in K14CreER:SmoM2 and K14CreER:SmoM2:Sox9cKO mice 9 weeks after TAM administration.

(B) Quantification of the number of apoptotic cells (Casp3+SmoM2+/SmoM2+) in K14CreER:SmoM2 and K14CreER:SmoM2:Sox9cKO mice 4, 9, and 16 weeks after TAM administration (n ≥ 4,058 cells counted per time point).

(legend continued on next page)

Sox9 Promotes Self-Renewing Division in SmoM2-Expressing Cells

To determine the cellular mechanisms leading to the disappearance of SmoM2-expressing cells in the absence of *Sox9*, we first assessed whether *Sox9* deletion increased apoptosis in SmoM2-expressing cells (Figures 2A and S2A). No increase in the number of active caspase-3-positive cells was observed at any time point following SmoM2 expression and *Sox9* deletion (Figure 2B), showing that Sox9 does not inhibit apoptosis in oncogene-expressing cells.

We next investigated whether the loss of *Sox9* induces a decrease in proliferation of oncogene-expressing cells, leading to their outcompetition by WT cells. Examination of Ki67 immunostaining revealed that *Sox9* deletion did not lead to a decrease in the proliferation of SmoM2-expressing cells (Figures 2C and S2B). On the contrary, proliferation of SmoM2-expressing cells was increased in absence of *Sox9* (Figure 2D), suggesting that Sox9 could promote quiescence rather than proliferation in oncogene-expressing cells.

Because the loss of SmoM2+ cells was not due to increased apoptosis or decreased proliferation, we assessed the possibility that Sox9 regulates the balance between self-renewal and differentiation during tumorigenesis. During homeostasis, IFE progenitors divide asymmetrically at the population level, giving rise on average to one basal K5+ cell and one differentiated suprabasal K1+ cell (Clayton et al., 2007; Mascré et al., 2012). However, upon SmoM2 expression, basal IFE progenitors stop dividing asymmetrically and differentiating into suprabasal IFE cells and instead accumulate into basal-like lesions that progressively invade the dermis (Youssef et al., 2012; Youssef et al., 2010). During epidermal development, the orientation of the spindle poles perpendicular to basal lamina (BL) promotes skin stratification (Lechler and Fuchs, 2005). We thus assessed the orientation of the spindle poles following SmoM2 expression and *Sox9* deletion by measuring the angle between the two centrosomes (NuMA) and BL. At 4 weeks following TAM, SmoM2-expressing basal IFE basal cells divided most frequently perpendicular to the BL irrespective of Sox9 expression (Figures 2E and 2F). In contrast, the transition from dysplasia or hyperplasia to BCC was accompanied by an increase in parallel division, which was further enhanced in fully invasive BCC (Figure 2F). Interestingly, this switch from perpendicular to parallel cell division was prevented by *Sox9* deletion (Figure 2F). Although deletion of Sox9 did not affect the apicolateral polarity of Par3 (Figure S2D), the segregation of Par3 in dividing (PH3+) cells further supports the increase of symmetric cell division that accompanied the progression from dysplasia to BCC (Figures S2E and S2F).

To assess more directly whether Sox9 regulates the fate of oncogene-expressing cells, we performed short-term lineage tracing using 5-ethynyl-2′-deoxyuridine (EdU) pulse-chase experiments at 4 and 9 weeks following TAM administration. To that end, we administrated EdU and analyzed the cells that initially incorporated EdU and the fate and localization of their progeny 24 hr after EdU administration (chase) (Figure S2C). After 4 hr, all EdU+ cells were located along the BL (Figures 2G–2I). At 4 weeks following TAM administration, many EdU+ cells were found in suprabasal differentiated cells after 24 hr of chase (Figures 2G and 2I), consistent with the majority of asymmetric cell division at this stage. In contrast, at 9 weeks following TAM, in the presence of *Sox9*, the majority of SmoM2+ IFE cells gave rise to two basal cells, whereas in the absence of *Sox9*, many EdU+ cells were found in suprabasal differentiated cells, as at 4 weeks (Figures 2G–2I), indicating that Sox9 inhibits asymmetric cell fate outcome of oncogene-expressing cells during tumor progression.

The decrease in symmetric division following *Sox9* deletion was accompanied by an increase production of differentiated cells, as shown by the proportional increase of K1+ differentiated cells in *Sox9*-deficient cells (Figures 2J and 2K). Altogether, these data indicate that Sox9 controls the balance between symmetric and asymmetric cell division during skin tumorigenesis and consequently the long-term maintenance of oncogene-expressing cells.

Identification of Sox9 Direct Target Genes in BCC

To determine the molecular mechanisms by which Sox9 regulates BCC formation, we assessed the molecular changes associated with *Sox9* deletion in SmoM2-expressing cells. To that end, we purified SmoM2-expressing cells using fluorescence-activated cell sorting (FACS) 9 weeks following TAM administration and performed microarray analysis of SmoM2-expressing cells in the presence or in the absence of *Sox9*. Microarray confirmed by RT-PCR analysis showed that all classical HH target genes, such as *Gli1*, *Gli2*, *Ptch1*, and *Ptch2*, were upregulated by SmoM2 regardless of *Sox9* expression (Figure 3A; Table S1), showing that Sox9 does not regulate HH signaling during BCC initiation. No difference in the expression of Wnt ligands, Wnt receptors, or their target genes, such as *Lef1* and *Bgn*, were observed in SmoM2-expressing cells deficient for Sox9 (Figures 3A and S3A), showing that Sox9 does not control the activation of Wnt/β-catenin signaling mediated by SmoM2

(C) IF of SmoM2 and Ki67 in K14CreER:SmoM2 and K14CreER:SmoM2:Sox9cKO mice 9 weeks after TAM administration.
(D) Quantification of the proliferative cells (Ki67+SmoM2+/SmoM2+) in K14CreER:SmoM2 and K14CreER:SmoM2:Sox9cKO mice 4, 9, and 16 weeks after TAM administration ($n \geq 8{,}721$ cells counted per time point from $n \geq 4$ different mice).
(E) IF showing the method used to measure the angle between the two centrosomes (NuMA) and the BL (β4 integrin).
(F) Quantification of the angle of cell division in K14CreER:SmoM2 and in K14CreER:SmoM2:Sox9cKO mice ($n \geq 132$ total cells counted per genotype in five different mice).
(G) IF of EdU and LamV showing incorporation of EdU after a 4 hr pulse and a 24 h pulse-chase.
(H and I) Quantification of the basal and suprabasal EdU-positive cells after an EdU pulse (4 hr) and a pulse-chase (24 hr) ($n \geq 4{,}055$ cells counted per time point from n = 3 different mice).
(J) IF for the differentiation marker K1 and SmoM2.
(K) Quantification of the percentage of differentiated cells (K1+SmoM2+/SmoM2+) in K14CreER:SmoM2 and in K14CreER:SmoM2:Sox9cKO mice 4 and 9 weeks after TAM administration ($n \geq 3{,}971$ cells counted per time point from $n \geq 6$ different mice).
Data represent the mean and SEM of at least three biological replicates. *$p \leq 0.05$; **$p \leq 0.01$; ***$p \leq 0.001$. The scale bars represent 50 μm.

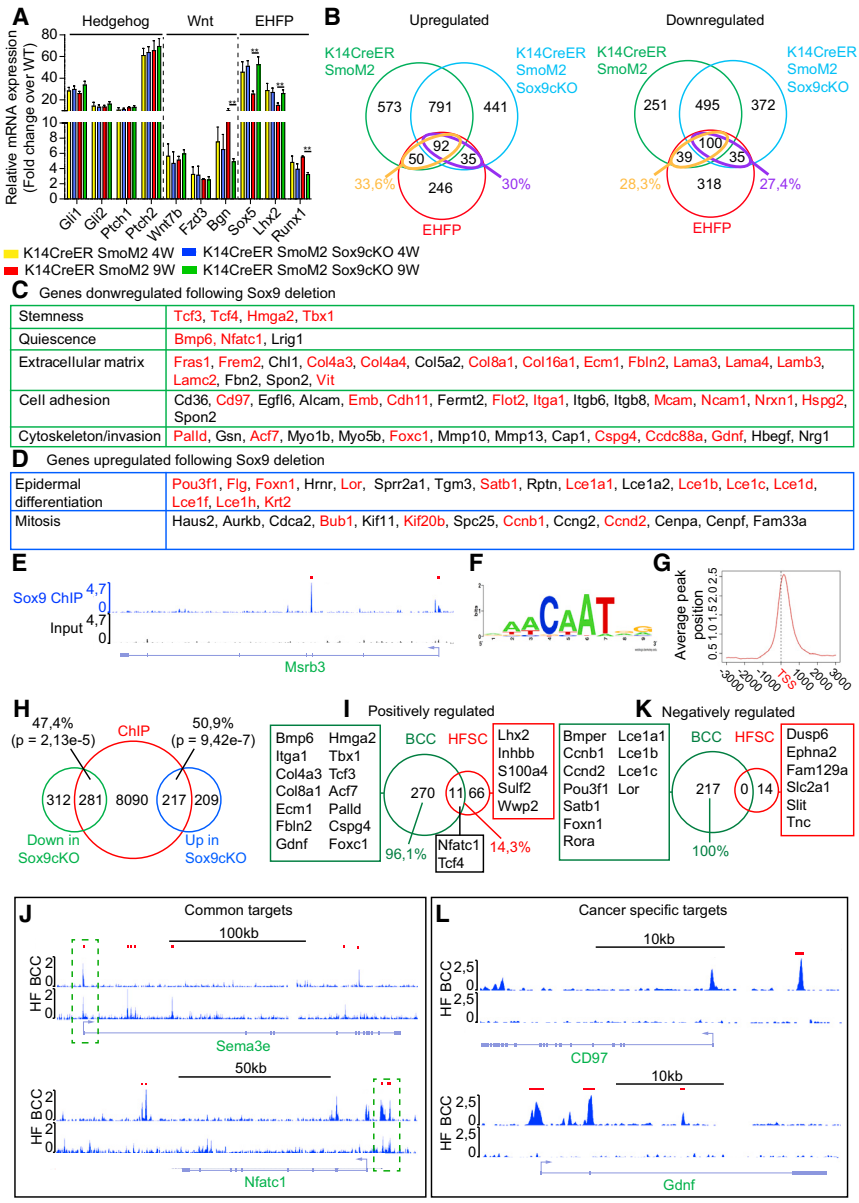

Figure 3. Sox9 Activates and Represses Gene Expression during Tumorigenesis

(A) Relative mRNA expression of genes involved in HH signaling, Wnt signaling, and the EHFP signature in FACS-isolated cells from K14CreER:SmoM2 and in K14CreER:SmoM2:Sox9cKO 9 weeks after TAM administration assessed by qRT-PCR. Fold changes were calculated over WT using the delta delta CT method after normalization over TBP. Data represent the mean and SEM of at least three biological replicates.

(B) Venn diagrams of the EHFP, adult IFE SmoM2+, and SmoM2:Sox9cKO gene signatures. Signatures are generated by taking the genes with fold changes higher or lower than +2 and −2, respectively, compared with WT IFE in two biologically independent microarray analyses.

(C and D) Table showing a list of genes (C) downregulated or (D) upregulated by more than 2-fold 9 weeks after TAM administration. Genes in red are putative direct Sox9 target genes as determined by ChIP-seq.

(E) Example of peak associated with Msrb3 in ChIP-seq (blue track) and input DNA (black track). Red bar denotes MACS peak position; gene is represented in light blue, and boxes represent exons. Arrow represents transcription orientation.

(F) Sox9 canonical motif, enriched in 60.25% of the peaks identified.

(G) Average profile of ChIP peaks relative to TSS.

(H) Venn diagram representing the merge between genes downregulated following Sox9 depletion (green), genes upregulated following *Sox9* deletion (blue) in microarray expression, and genes that are associated with a least one peak in ChIP-seq (red).

(I) Venn diagrams representing the genes directly upregulated by Sox9 in BCC (green) and HFSCs (red) (Kadaja et al., 2014).

(J) Common Sox9 targets in HFSCs and BCC. Red bar denotes MACS peak position; gene is represented in light blue, and boxes represent exons. Arrow represents transcription orientation.

(K) Venn diagrams representing the genes directly downregulated by Sox9 in BCC (green) that showed no overlap with HFSCs (Kadaja et al., 2014).

(L) Tumor-specific Sox9 target genes. Red bar denotes MACS peak position; gene is represented in light blue, and boxes represent exons. Arrow represents transcription orientation.

*p ≤ 0.05; **p ≤ 0.01; ***p ≤ 0.001.

expression. Similarly, microarray analysis, RT-PCR and immunostaining showed no difference in the upregulation of EHFP genes such as *Lhx2*, *Cux1*, *Pcadh*, and *Runx1* in SmoM2-expressing cells deficient for *Sox9* (Figures 3B and S3A–S3D). Altogether these data show that Sox9 does not control HH and Wnt/β-catenin activation or the initial reprogramming of adult IFE cells into EHFP-like fate during BCC initiation.

Our microarray analysis showed that *Sox9* deletion induced the downregulation of 593 genes and the upregulation of 447 genes by more than 2-fold in two independent biological experiments (Figures 3C and 3D; Table S1). *Sox9* deletion in SmoM2-expressing cells induced a decrease in the expression of genes promoting stemness (e.g., *Tcf3*, *Tcf4*, *Hmga2*, *Tbx1*) (Chen et al., 2012; Nguyen et al., 2009; Nishino et al., 2008), quiescence (e.g., *Nfatc1*, *Lrig1*, *Bmp6*) (Blanpain et al., 2004; Horsley et al., 2008; Jensen and Watt, 2006), ECM (e.g., *Col4a4*, *Col16a1*, *Lama3*, *Lamc2*), cell adhesion (e.g., *Itga1*, *Itgb6*, *Emb*, *Mcam*), cytoskeleton remodeling (e.g., *Palld*, *Gsn*, *Acf7*), and invasion (e.g., *Mmp10*, *Mmp13*, *Foxc1*), as well as an increase in the expression of genes regulating proliferation (e.g., *Ccnb1*, *Ccnd2*, *Cdca2*) and IFE differentiation (e.g., *Lor*, *Fil*, and genes belonging to the epidermal differentiation complex [EDC]).

To determine which of these differentially regulated genes represent direct target genes, we performed Sox9 ChIP-seq in primary BCCs induced by SmoM2 expression (Figure 3E). We first identified the regions that were significantly enriched in the Sox9 ChIP compared with the input DNA using MACS peak-calling software with the false discovery rate (FDR) set to 5% (see

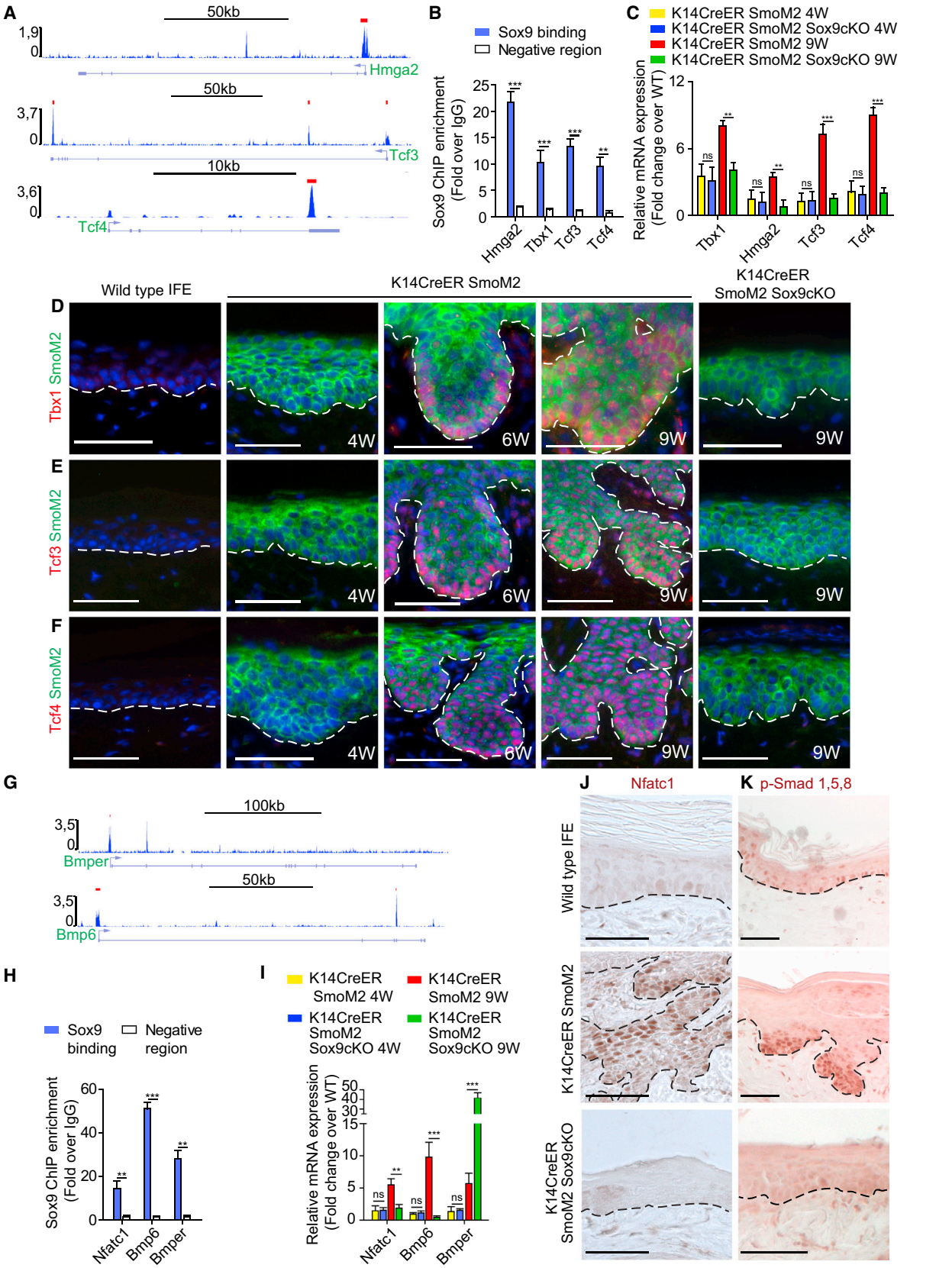

(legend on next page)

Experimental Procedures for further details) and defined the genes displaying at least one Sox9 peak within the gene and the 50 kb region surrounding the coding sequence.

Motif analysis revealed that 60.25% of the ChIP peaks identified contained the canonical Sox9 motif "AACAAT" (Figure 3F) (Lefebvre et al., 1997), and these peaks were preferentially clustered around the transcription start site (TSS) (Figure 3G). Interestingly, 47.4% of the downregulated genes and 50.9% of genes upregulated following *Sox9* depletion were directly bound by Sox9 (Figure 3H), supporting the notion that Sox9 acts as both transcriptional activator and repressor during tumorigenesis (Figures 3I–3L), contrasting with its mainly transcriptional activator function in HFSCs (Kadaja et al., 2014). Among the 77 genes downregulated upon *Sox9* loss of function and directly bound by Sox9 in adult HFSCs, 11 genes (14.3%) were commonly directly positively regulated by Sox9 during HF homeostasis and BCC (e.g., *Nfatc1*, *Sema3e*, *Tcf7l2*/*Tcf4*), which represent only 3.9% of the 239 genes upregulated and directly bound by Sox9 during tumorigenesis (Figures 3I and 3J). In contrast to HFSCs (Kadaja et al., 2014), Sox9 did not regulate the expression of Activin, Fzd receptors, or *Lhx2*, a key regulator of HF fate (Rhee et al., 2006) (Figures 3A and S3B). In addition, none of the 14 genes that were upregulated by *Sox9* deletion and bound by Sox9 in adult HFSCs were upregulated in HFSCs following *Sox9* deletion (Figures 3K and 3L). Sox9 has been proposed to act as pioneered binding at super-enhancers (SEs) in HFSCs (Adam et al., 2015). In HFSCs, Sox9 binds to 46% of SEs (174 of 374), whereas only 24% (89 of 374) of HFSC SEs were bound by Sox9 in BCCs, corresponding to less than 0.5% of Sox9 peaks in BCC. Among the genes presenting Sox9 peaks in HFSC SEs, 9% were deregulated by *Sox9* deletion in HFSC (e.g., Lhx2), whereas only 2% of the genes containing these SEs were deregulated by *Sox9* deletion in BCCs (e.g., Nfatc1), suggesting that Sox9 preferentially binds these SEs and that they are more functionally important in HFSC than in BCC. These data demonstrate that although some of the molecular mechanisms controlled by Sox9 in HFSCs (Kadaja et al., 2014) are partially reused during BCC formation, Sox9 presents a broader and different set of direct target genes during tumorigenesis, possibly related to its higher expression (Figure S3F) or to specific cooperating factors (Figure S3G) and presents a unique repressive function during tumorigenesis.

Sox9 Directly Regulates Genes Promoting SC Renewal and Quiescence

Our microarray and ChIP-seq analyses, confirmed by ChIP-qPCR and qRT-PCR experiments showed that Sox9 directly promoted the expression of several well-known regulators of stemness, including *Hmga2* (Nishino et al., 2008), *Tbx1* (Chen et al., 2012), and *Tcf3* and *Tcf4* (Nguyen et al., 2009) (Figures 4A–4C). Immunostaining showed that Hmga2, Tbx1, Tcf3, and Tcf4 were expressed as dysplasia progressed into BCCs but were absent following *Sox9* deletion (Figures 4D–4F and S4A). In addition, the expression of these genes co-localized with Sox9 in human BCCs, supporting the notion that Sox9 regulates the expression of stemness genes in human cancer as well (Figures S4B–S4D). These data indicate that in BCC Sox9 directly controls the expression of key genes promoting stemness.

Interestingly, Sox9 negatively regulated cell proliferation by directly regulating the expression of Bmp-Nftac1 axis that promotes HFSC quiescence (Blanpain and Fuchs, 2009; Blanpain et al., 2004; Horsley et al., 2008) (Figures 4G–4J). *Nfatc1* was directly induced by Sox9 in both HFSC and BCC at some common regulatory regions (Figures 3J, 4H, and 4I). In contrast, *Bmp6*, which promotes the quiescence of normal HFSC (Blanpain et al., 2004), was directly activated by Sox9 in BCC but not in HFSCs (Figures 4G–4I). *Bmper*, a potent inhibitor of Bmp signaling (Moser et al., 2003) was also directly bound by Sox9 in BCC and was strongly upregulated following *Sox9* deletion (Figures 4G–4I). The number of pSmad1/5/8 positive cells was strongly reduced in SmoM2-expressing cells following *Sox9* deletion (Figure 4K), showing the essential role of Sox9 in regulating the activation of the Bmp-Nfatc1 axis during skin tumorigenesis.

Sox9 Directly Represses Genes Controlling Epidermal Differentiation during BCC Initiation

Sox9 deletion in oncogene-expressing cells resulted in the upregulation of many key regulators of IFE differentiation, such as *Satb1* (Fessing et al., 2011), *Pou3f1*(Faus et al., 1994), *Rora*, and *Foxn1* (Dai et al., 2013), as well as many genes belonging

Figure 4. Sox9 Activates the Expression of Stemness Genes during Tumorigenesis

(A) Sox9 peaks in the regulatory regions of Hmga2, Tcf3, and Tcf4. Red bar denotes MACS peak position; gene is represented in light blue, and boxes represent exons. Arrow represents transcription orientation.

(B) PCR quantification of Sox9 ChIP in the regulatory regions of Hmga2, Tbx1, Tcf3, and Tcf4. Sox9 ChIP is normalized over control IgG. Sox9-binding primers (blue) are designed within the peak, while negative region primers (white) are designed 2 kb upstream of the peak.

(C) qPCR analysis showing relative mRNA expression of Tbx1, Hmga2, Tcf3, and Tcf4 in FACS-isolated cells from K14CreER:SmoM2 and in K14CreER:SmoM2:Sox9cKO 4 and 9 weeks after TAM administration. Fold changes were calculated over WT using the delta delta CT method after normalization over TBP. Data represent the mean and SEM of at least 3 biological replicates.

(D–F) IF for SmoM2 and (D) Tbx1, (E) Tcf3, and (F) Tcf4, in K14CreER:SmoM2 and K14CreER:SmoM2:Sox9cKO mice 4, 6, and 9 weeks after TAM administration.

(G) Sox9 peaks for Bmp6 and Bmper. Red bar denotes MACS peak position; gene is represented in light blue, and boxes represent exons. Arrow represents transcription orientation.

(H) Quantification of the enrichment following immunoprecipitation for Nfatc1, Bmper, and Bmp6. Enrichment is normalized over control IgG. Sox9-binding primers (blue) are designed within the peak, while negative region primers (white) are designed 2 kb upstream of the peak.

(I) qPCR analysis of Nfatc1, Bmp6, and Bmper on FACS-isolated cells from K14CreER:SmoM2 mice and in K14CreER:SmoM2:Sox9cKO mice 4 and 9 weeks after TAM administration. Data are normalized over WT.

(J) Immunohistochemistry (IHC) showing expression of Nfatc1 in K14CreER:SmoM2 but not in K14CreER:SmoM2:Sox9cKO mice 9 weeks after TAM administration.

(K) IHC for phosho-Smad1/5/8 in WT, K14CreER:SmoM2, and K14CreER:SmoM2:Sox9cKO mice.

The scale bars represent 50 μm. Data represent the mean and SEM of at least three biological replicates. *$p \leq 0.05$; **$p \leq 0.01$; ***$p \leq 0.001$.

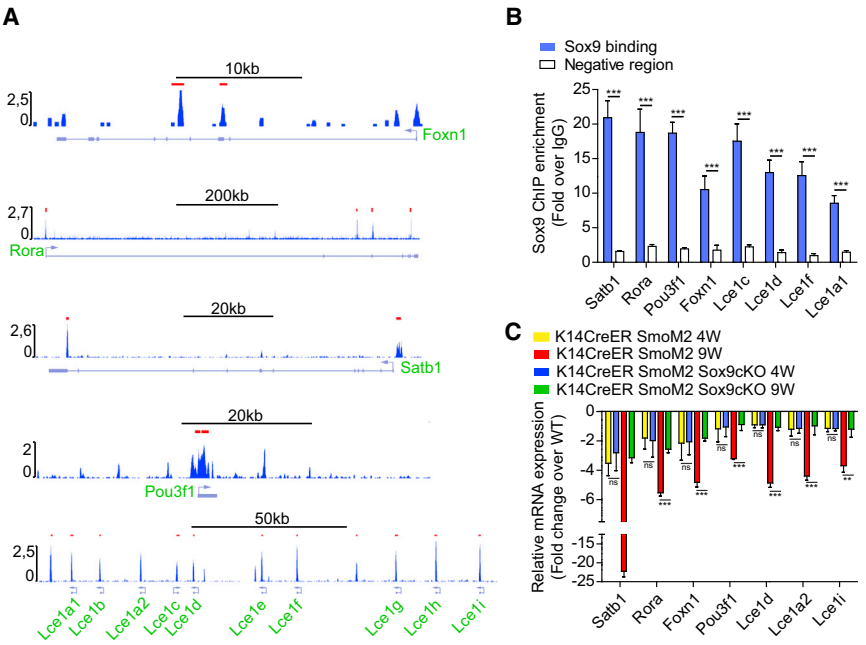

Figure 5. Sox9 Directly Represses Differentiation during Tumorigenesis

(A) Sox9 peaks associated with Foxn1, Rora, Satb1, Pou3f1, and a part of the EDC. Red bar denotes MACS peak position; gene is represented in light blue, and boxes represent exons. Arrow represents transcription orientation.

(B) PCR quantification of Sox9 ChIP in the regulatory regions of Foxn1, Satb1, Rora, Lce1d, Lce1c, and Lce1a1 genes. Enrichment is normalized over control IgG. PCR primers (blue) are designed within the peak and 2 kb upstream of the peak for negative controls.

(C) RT-qPCR analysis of key regulators of IFE differentiation (Satb1, Rora, Foxn1, Pou3f1) and genes belonging to the EDC (Lce1d, Lce1a2, and Lce1i) in FACS-isolated cells from K14CreER:SmoM2 mice and in K14CreER:SmoM2:Sox9cKO mice 4 and 9 weeks after TAM administration. Fold changes were calculated over WT using the delta delta CT method after normalization over TBP.

Data represent the mean and SEM of at least three biological replicates. Data represent the mean and SEM of at least three biological replicates. *p $\leq$ 0.05; **p $\leq$ 0.01; ***p $\leq$ 0.001.

to the EDC, a locus containing many genes that regulate epidermal differentiation such late cornified envelope (Lce) proteins (Candi et al., 2005) (Figure 3D). ChIP-seq experiments confirmed by ChIP-qPCR analysis showed that Sox9 directly repressed the expression of these genes (Figures 5A–5C), suggesting that Sox9 inhibits IFE differentiation upon SmoM2 expression, by directly repressing the expression of key transcriptional factors that promote epidermal differentiation and many genes of the EDC.

Sox9 Directly Controls ECM Remodeling, Cell Adhesion, and Actin Cytoskeleton during Initiation

Transcriptional analysis and ChIP experiments revealed that Sox9 positively regulated the expression of many components of the ECM and cell adhesion, including collagens (e.g., *Col4a3*, *Col4a4*), laminins (e.g., *Lama3*, *Lamb3*), integrins (e.g., *Itga6*, *Itgb6*, and *Itgb8*), and adhesion proteins (e.g., *Alcam*, *Mcam*), many of which were directly bound by Sox9 (Figures 3C and 6A–6C). Immunofluorescence (IF) and FACS analysis confirmed the upregulation of several key components of the BL (e.g., Col4) and adhesion proteins (e.g., Itga6, Mcam), as SmoM2-expressing cells progressed from dysplasia to invasive BCC, while *Sox9* deletion prevented these changes (Figures 6D–6F, S5A, and S5B). To analyze more precisely how Sox9 regulates cell adhesion and ECM deposition, we performed electron microscopy (EM) analysis 9 weeks following SmoM2 expression in the presence or in the absence of *Sox9*. ECM was more fragile following *Sox9* deletion, resulting in a number of gaps between the collagen fibers; the BL was thinner; and the cell-cell adhesions were severely impaired, with multiple gaps between cells (Figures 6G and S5C–S5E). Using second harmonic generation (SHG), we analyzed the structure and orientation of type I and II collagen fibrils and found that progression from dysplasia to invasive BCC is accompanied by a reorganization of the ECM with highly organized thick collagen fibers surrounding the tumorigenic lesions (Figure 6D). In contrast, the collagen fibers were disorganized upon *Sox9* deletion, indicating the essential role of Sox9 in mediating ECM remodeling during tumorigenesis (Figure 6D).

The recruitment of inflammatory cells in the tumor stroma plays a critical role during tumor invasion and progression. Although our transcriptional profiling and ChIP-seq data did not provide evidence that Sox9 directly controls inflammation and immunity, we have assessed the presence of immune and inflammatory cells (CD45: pan-hematopoietic marker; F4/80: monocyte marker; GR1: granulocyte marker; and CD3: T cell marker) following SmoM2 expression and *Sox9* deletion. At dysplasia stage (4 weeks) and during BCC progression (6 weeks), no differences in the number of inflammatory cells underlying SmoM2-expressing cells were observed in the presence or absence of Sox9 (Figures S6A–S6E). However, an increase in the number of inflammatory cells, in particular monocytes and macrophages, was observed at the stromal interface of the leading edge of invasive BCC lesions (Figures S6A–S6E), whereas at the same time point, many fewer immune and inflammatory cells were observed in Sox9-deficient SmoM2-expressing cells, suggesting that the recruitment of inflammatory cells is associated with later stage of BCC progression and that Sox9 may indirectly regulate this process.

Importantly, we found that Sox9 regulated directly and indirectly the expression of key regulators of actin cytoskeleton dynamics, which are essential for cell migration and invasion (Figures 3C and 6H–6K). F-actin transduces the mechanical force between the contractile cytoskeleton and the ECM to allow cell migration. Gelsolin (*Gsn*), an actin filament severing and capping protein, which promotes actin polymerization (Witke et al., 1995), was profoundly downregulated upon *Sox9* deletion in SmoM2-expressing cells (Figure 6J), although no peaks were found within 50 kb surrounding *Gsn* start site in Sox9 ChIP-seq. In contrast, Sox9 directly promoted the expression of Palladin

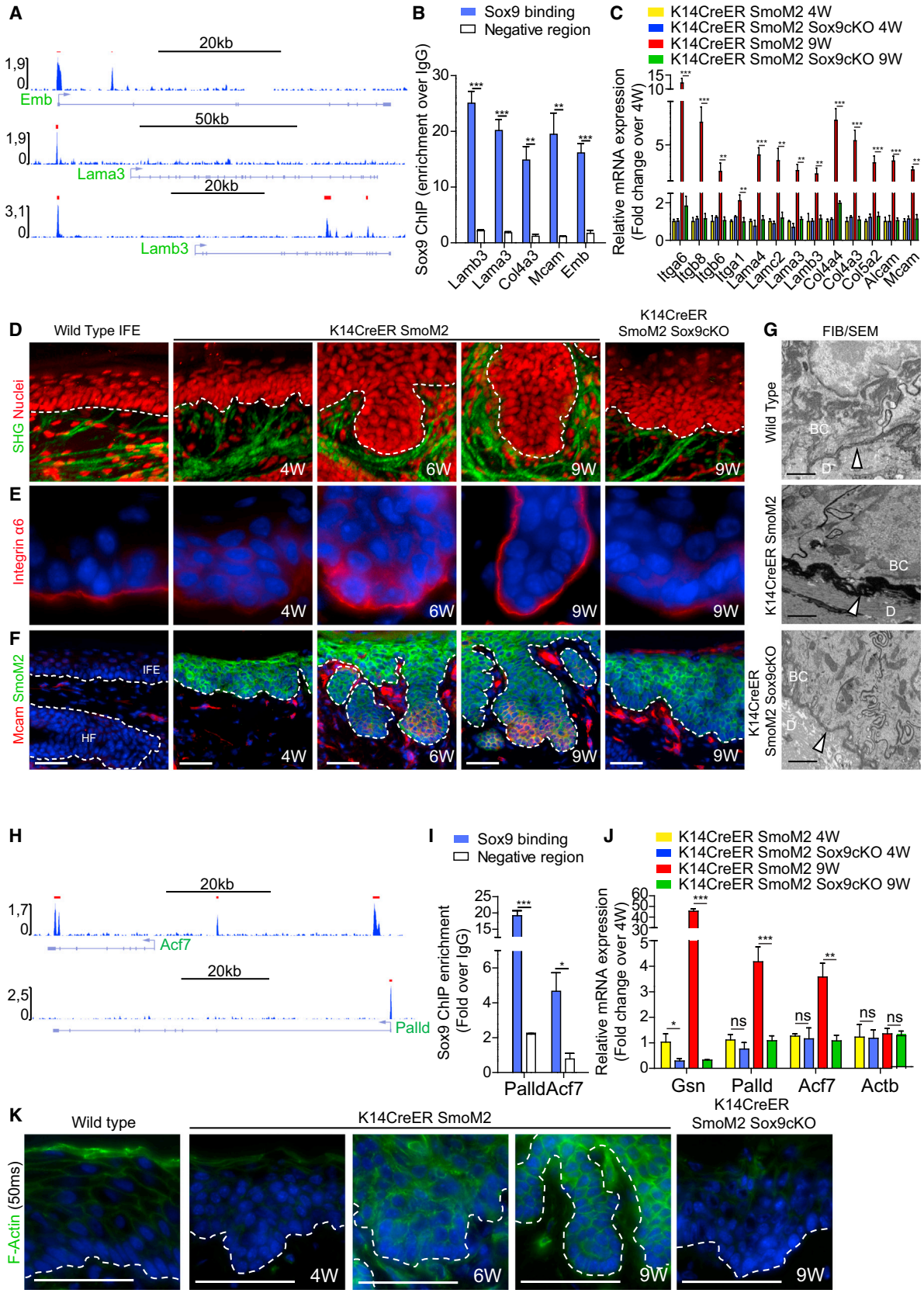

(legend on next page)

(*Palld*) (Figures 6H–6J), which directly binds to F-actin, and crosslink actin filaments into bundles and acts as a scaffold that recruits actin-binding protein to promote cell motility (Goicoechea et al., 2008; Najm and El-Sibai, 2014). Finally, Sox9 also regulates the expression of *Macf1*/*Acf7* (Figures 6H–6J), a microtubule-actin crosslinking protein that connects the microtubule and the actin cytoskeleton and promotes the migration of HFSCs (Wu et al., 2011).

To determine the functional role of Sox9 and its target genes in the regulation of actin polymerization and bundling during BCC progression, we analyzed the levels of F-actin during SmoM2-induced tumorigenesis. Tumor progression from dysplasia to BCC was accompanied by an increase in polymerized actin (Figure 6K). Similarly in human BCCs, F-actin was also increased in BCC, compared with the adjacent normal skin epidermis (Figure S5F). However, in the absence of *Sox9*, while actin mRNA was unchanged (Figure 6J), no increase in F-actin was observed following SmoM2 expression (Figure 6K), demonstrating the key role of Sox9 in regulating actin polymerization during tumor initiation. Altogether, these data reveal that Sox9 directly regulates ECM deposition, cell adhesion, and actin cytoskeleton reorganization that accompany the early steps of BCC invasion.

DISCUSSION

Although Sox9 is expressed in many human cancers, little is known about the molecular mechanisms by which Sox9 regulates tumorigenesis. Here, we show that Sox9 is rapidly upregulated during the early steps of BCC initiation in a Wnt/β-catenin-dependent manner and is essential for the long-term self-renewal of oncogene-expressing cells and their acquisition of invasive properties. Transcriptional profiling combined with ChIP-seq uncovers a GRN directly regulated by Sox9 that plays an essential role in promoting self-renewing division and repressing the normal differentiation program of oncogene targeted cells, as well as regulating ECM and cytoskeleton remodeling required for tumor invasion (Figure 7).

Similarly to what was found during pancreas and prostate cancer development (Kopp et al., 2012; Thomsen et al., 2010), Sox9 is expressed at the early steps of BCC initiation and is essential for tumor formation. During pancreatic cancer development, it has been proposed that Sox9 promotes the reprogramming of acinar cells into ductal-like cells upon KRasG12D expression followed by pancreas injuries (Kopp et al., 2012). In contrast, during BCC formation, Sox9 is not required for the initial reprogramming step of adult IFE cells into EHFPs but is critical for the long-term maintenance of oncogene-expressing cells, reminiscent of its role during HFSC homeostasis (Nowak et al., 2008; Vidal et al., 2005) and for tumor invasion. Surprisingly, the progressive loss of *Sox9*-deficient oncogene-expressing cells was not due to an increase in apoptosis or a decrease in cell proliferation. On the contrary, the proliferation was even further increased following *Sox9* deletion, most probably because of the loss of *Sox9*-mediated relative quiescence mediated by the Bmp/Nfatc1 axis.

Although Sox9 overexpression in human keratinocytes or mouse epidermis promotes cell growth and inhibits epidermal differentiation (Adam et al., 2015; Shi et al., 2013), as it does during BCC development, Sox9 overexpression alone does not appear to promote tumor formation (Adam et al., 2015; Shi et al., 2013), suggesting that other pathways beside Sox9 activation are required downstream of oncogenic HH/Wnt-signaling axis to promote BCC development. Transcriptional profiling of oncogene-expressing cells deficient for *Sox9* combined with ChIP-seq uncovered a GRN controlled by Sox9 during BCC formation. Although some of the Sox9 target genes, such *Tcf3* or *Nfatc1*, are commonly regulated by Sox9 in BCC and HFSC homeostasis, Sox9 regulates a unique GRN during skin tumorigenesis. The most striking difference in the molecular mechanisms controlled by Sox9 in HFSCs and BCC, is the dual transcriptional activator and repressor functions of Sox9 during tumorigenesis, while Sox9 acts mainly as a transcriptional activator in HFSCs (Kadaja et al., 2014). During BCC carcinogenesis, Sox9 directly inhibits the expression of key transcriptional regulators of normal IFE differentiation such as *Satb1*, a TF essential for epidermal stratification and differentiation (Fessing et al., 2011), *Pou3f1*, which represses the expression of the basal keratins K14 and K5 during IFE differentiation (Faus et al., 1994), as well as *Foxn1* and *Rora* that promote IFE differentiation (Dai et al.,

Figure 6. Sox9 Directly Controls ECM, Adhesion, and Cytoskeleton Remodeling during Tumorigenesis

(A) Sox9 ChIP-seq peaks associated with Emb, Lama3, and Lamb3. Red bar denotes MACS peak position; gene is represented in light blue, and boxes represent exons. Arrow represents transcription orientation.

(B) PCR quantification of Sox9 ChIP in the regulatory regions of Lamb3, Lama3, Col4a3, Mcam, and Emb. Enrichment is normalized over control IgG. PCR primers are designed within the peak and 2 kb upstream of the peak for negative controls.

(C) qRT-PCR analysis of cell adhesion and ECM and cell adhesion genes in FACS-isolated cells from K14CreER:SmoM2 mice and in K14CreER:SmoM2:Sox9cKO mice 4 and 9 weeks after TAM administration. Fold changes were calculated over K14CreER:SmoM2 mice 4 weeks after TAM using the delta delta CT method after normalization over TBP. Data represent the mean and SEM of at least three biological replicates.

(D) SHG analyzed by multiphoton confocal microscopy in WT, K14CreER:SmoM2, and K14CreER:SmoM2:Sox9cKO mice 4, 6, and 9 weeks after TAM administration.

(E and F) Immunostaining of (E) α6 integrin and (F) Mcam and SmoM2 in K14CreER:SmoM2 mice and in K14CreER:SmoM2:Sox9cKO mice 4, 6, and 9 weeks after TAM administration.

(G) EM analysis of WT, K14CreER:SmoM2, and K14CreE:SmoM2:Sox9cKO mice 9 weeks after TAM administration. BC, basal keratinocytes; D, dermis.

(H) Sox9 peaks associated with Acf7 and Palld.

(I) PCR quantification of Sox9 ChIP in the regulatory regions of Palld and Acf7. Enrichment is normalized over control IgG.

(J) Relative mRNA expression of actin cytoskeleton regulators in FACS-isolated cells from K14CreER:SmoM2 mice and in K14CreER:SmoM2:Sox9cKO mice 4 and 9 weeks after TAM administration. Data are normalized over K14CreER:SmoM2 mice 4 weeks after TAM administration and represent the mean and SEM of at least three biological replicates.

(K) IF of filamentary actin (F-actin) stained with phalloidin in K14CreER:SmoM2 and K14CreER:SmoM2:Sox9cKO mice.

Exposure time is 50 ms for all acquisition. The scale bars represent 50 μm, except in (G), where it represents 100 nm. Data represent the mean and SEM of at least three biological replicates. *$p \leq 0.05$; **$p \leq 0.01$; ***$p \leq 0.001$.

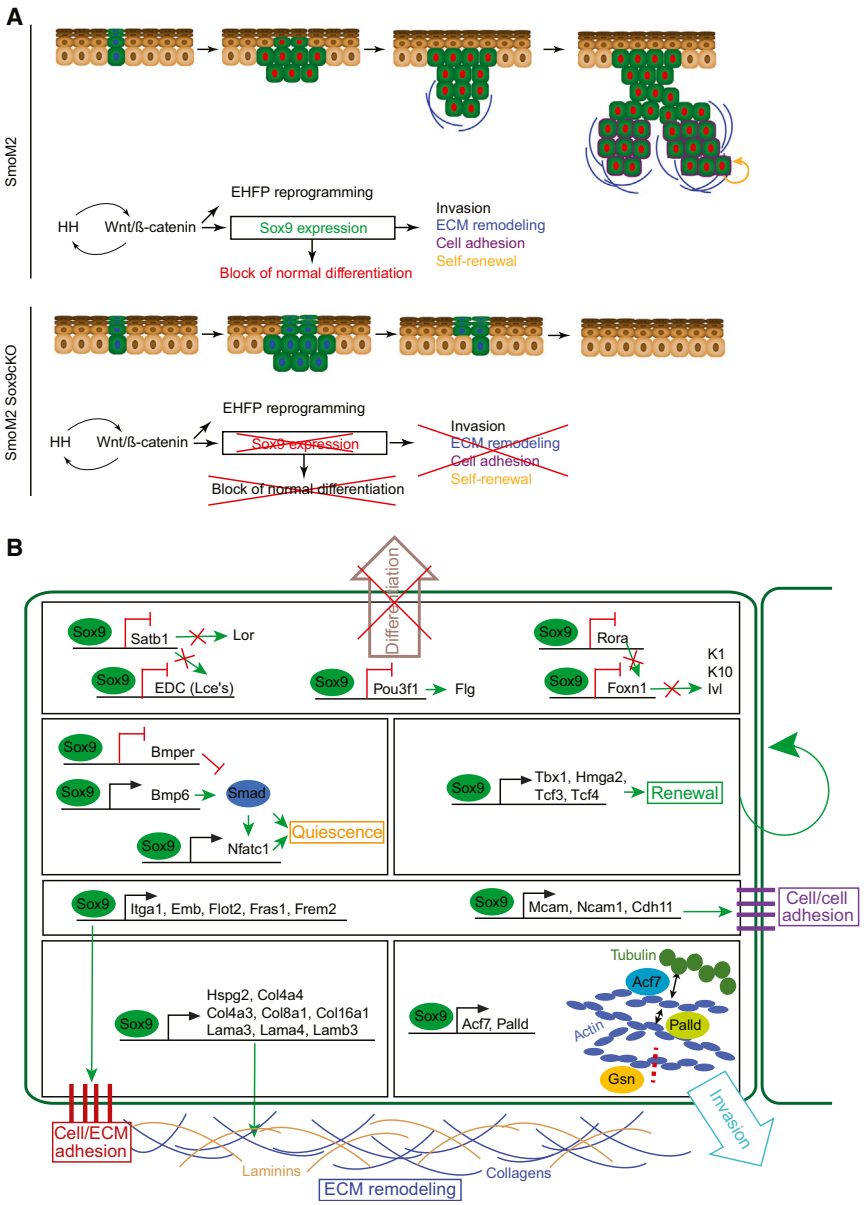

Figure 7. Mechanisms Regulated by Sox9 during Tumorigenesis

(A) Model summarizing the role of Sox9 in BCC formation.

(B) Schematic representation of the GRN underlying Sox9 functions in an oncogene-expressing cells. Sox9-mediated gene activation is represented by arrows while Sox9-mediated repression is represented by red bars. Cellular functions are enclosed in colored boxes.

2013). Moreover, Sox9 also directly inhibits the expression of genes encoding for structural proteins associated with epidermal terminal differentiation. The difference of Sox9 target genes in normal HFSC and BCC formation may be related to the higher level of Sox9 expression in BCC or, to the different epigenetic landscape and set of TFs such as Zfx, an essential gene for BCC formation (Palmer et al., 2014) that could cooperate with Sox9 to regulate gene expression in tumor cells.

In addition, to regulate the balance between self-renewal and differentiation in oncogene-expressing cells by directly promoting the expression of genes regulating stemness and repressing the expression of genes that mediate IFE differentiation, Sox9 can also regulate the long-term maintenance of oncogene-expressing cells by promoting the relative quiescence of tumor initiating cells, as the slow-growing nature is one of the hallmarks of BCC (Epstein, 2008). Sox9 promotes the relative quiescence of HFSCs and BCC-initiating cells by common and distinct mechanisms. In both situations, Sox9 directly promotes the expression of *Nfatc1*, a TF that regulates HFSC quiescence (Horsley et al., 2008). Bmp and Tgf-β signaling are two key pathways promoting quiescence in the epidermis (Blanpain and Fuchs, 2009). Although in HFSC, Sox9 promotes HFSC quiescence by directly stimulating the expression of activin leading to the activation of the Tgf-β pathway (Kadaja et al., 2014), during skin tumorigenesis, Sox9 regulates Bmp signaling by directly promoting the expression of Bmp6 and repressing the expression of Bmp inhibitor.

We found that invasion of BCC-initiating cells is associated with a profound remodeling of the ECM, cell adhesion, and actin cytoskeleton. Our molecular analysis revealed that Sox9 is a key regulator of the cellular and molecular changes associated with BCC invasion. Sox9 directly promotes the expression of key components of the ECM and the BL such as laminins, collagens, and molecules that promote adhesion to the ECM, such as integrins as well as cell-cell adhesion proteins expressed at the leading edge of invasive BCC. The decrease in the level of expression of several integrins, including a6 integrin, may also partially explain the progressive loss of oncogene-expressing cells deficient for Sox9. Indeed, α6 integrin is one of the most common upregulated genes across many different SCs (Fortunel et al., 2003) and in the skin IFE, a high level of integrins is associated with increased SC potential (Jones and Watt, 1993).

Sox9 regulates cytoskeleton dynamics that occurred during BCC invasion by directly controlling the expression of Palld, which promotes actin polymerization in tumor cells and Acf7, a molecule that regulates and coordinates actin cytoskeleton and microtubule dynamics and controls the migration of HFSCs (Wu et al., 2011), a physiological process reminiscent of the collective migration occurring during BCC invasion.

In conclusion, our study uncovers the cellular and molecular mechanisms, as well as the GRN regulated by Sox9 during the early steps of skin tumor initiation and demonstrates that Sox9

controls the long-term self-renewal of oncogene-expressing cells by promoting symmetric renewing division and inhibiting differentiation. In addition, Sox9 also acts as key orchestrator of the ECM remodeling, cell adhesion, and cytoskeleton dynamics required for tumor invasion (Figure 7). These results have important implications for the development of novel strategies to block formation and invasion in the most frequent cancer in humans.

EXPERIMENTAL PROCEDURES

Mice

Similar numbers of males and females were used for each experiment. Detailed information regarding mice strains and housing are reported in Supplemental Experimental Procedures. Experiments involving mice presented in this work were approved by Comité d'Éthique du Bien Être Animal (Université Libre de Bruxelles) under protocol number 483N. Experiments involving human samples presented in this work were approve by the ethics committee of Erasmus Hospital under protocol number P2012/332.

Immunostaining

Immunostaining was performed as described previously (Youssef et al., 2012). Detailed procedures are reported in Supplemental Experimental Procedures.

Light and Epifluorescence Microscopy

Images were acquired using an Axio Imager M1 microscope and an AxioCamMR3 or MrC5 (Carl Zeiss). For expression level comparison, all images were acquired at equal exposure.

Confocal Microscopy

Cryosections 30 μm thick were fixed in 4% paraformaldehyde and incubated overnight with 7AAD to label nuclei. Z-stacks of equal thickness were subjected to maximum-intensity projection using Zen Black (Carl Zeiss).

Detailed descriptions of all other microscopic procedures, transmission EM, and focused ion beam/scanning EM are available in Supplemental Experimental Procedures.

FACS Isolation of Oncogene-Expressing Cells

Isolation of keratinocytes and RNA extraction were performed as previously described (Youssef et al., 2012). Briefly, tail skin keratinocytes were isolated and stained with anti-CD34 and anti-α6 integrin antibodies. SmoM2-YFP+/α6+/CD34+ living cells, corresponding to IFE and infundibulum cells, were harvested directly into the lysis buffer before extraction was performed according to the manufacturer's instruction (RNeasy Mini Kit; Qiagen). Detailed procedures are reported in Supplemental Experimental Procedures.

Real-Time RT-PCR Analysis

qRT-PCR was performed as described previously (Youssef et al., 2012). Briefly, after RNA quantification using NanoDrop, the purified RNA was used to generate cDNA strand using SuperScript II polymerase (Invitrogen) and random hexamers (Roche). qPCR was performed using FastStart SYBR Green Master (Roche) on a LightCycler 96 device (Roche). Fold changes were calculated using the delta delta CT method after normalization over TBP. The list of primers used is reported in Table S5.

ChIP-seq

Ten million keratinocytes isolated from tail epidermis of K14CreER:SmoM2 mice 9 weeks after TAM administration were crosslinked for 10 min with 1% formaldehyde on a rotating wheel. The reaction was quenched by adding 0.125 M glycine and washed twice in PBS. ChIP was performed using the EZ-Magna ChIP kit (Millipore) according to the manufacturer's instruction for all steps except lysis, which was carried using SDS lysis buffer (Millipore). The chromatin was sonicated into 300 to 500 bp fragments using a Bioruptor (Diagenode) coupled to a cooling system to maintain temperature at about 4°C. Antibodies used for ChIP were Sox9 (Ab5535; Millipore) and control immunoglobulin G (IgG) (Ab46540; Abcam).

Five to ten nanograms of ChIPed DNA were subjected to library preparation using the TruSeq ChIP Sample Prep Kit (Illumina), with small variations described in Supplemental Experimental Procedures and sequenced on a HiScanSQ module (Illumina).

ChIP Analysis

Briefly, unique mapped reads were aligned on mouse genome (NCBI Build 37/UCSC mm9), and peaks were discovered using MACS software (version 1.4) using an FDR threshold of 5% and a minimal fold enrichment of 2. Detailed procedures are described in Supplemental Experimental Procedures.

Microarray Analysis

RNA from FACS-purified cells was labeled and hybridized on a mouse genome 430 2.0 array (Affymetrix) by AROS Applied Biotechnology A/S. Biological duplicates were performed for both K14CreER:SmoM2 and K14CreER:SmoM2:Sox9cKO mice 9 weeks after induction. We considered genes upregulated or downregulated by more than 2-fold in two independent biological duplicates.

ACCESSION NUMBERS

The accession number for the microarray data reported in this paper is GEO: GSE68613. The accession number for the ChIP-seq data reported in this paper is GEO: GSE68755.

SUPPLEMENTAL INFORMATION

Supplemental Information includes Supplemental Experimental Procedures, six figures, and five tables and can be found with this article online at http://dx.doi.org/10.1016/j.stem.2015.05.008.

ACKNOWLEDGMENTS

We thank the animal house facility from Université Libre de Bruxelles (ULB) (Erasme campus). We thank Sylvain Brohée (Jules Bordet Institute) for his help with the bioinformatics analysis. We thank Hoang Nguyen (Baylor College of Medicine) for providing us with Tcf3 antibody. C.B. is an investigator of WELBIO. J.-C.L. is supported by a fellowship from Fonds de la Recherche Scientifique (FNRS)/Fonds pour la Formation à la Recherche dans l'Industrie et dans l'Agriculture. B.D. is supported by a fellowship from FNRS. A.S.-D. is supported by a Chargé de Recherche grant from FNRS. This work was supported by FNRS, Télévie, the PAI program, a research grant from Fondation Contre le Cancer, ULB Fondation, Fond Gaston Ithier, the Fondation Bettencourt Schueller, Fondation Baillet-Latour, and the European Research Council.

Received: November 13, 2014
Revised: March 30, 2015
Accepted: May 15, 2015
Published: June 18, 2015

REFERENCES

Adam, R.C., Yang, H., Rockowitz, S., Larsen, S.B., Nikolova, M., Oristian, D.S., Polak, L., Kadaja, M., Asare, A., Zheng, D., and Fuchs, E. (2015). Pioneer factors govern super-enhancer dynamics in stem cell plasticity and lineage choice. Nature *521*, 366–370.

Blanpain, C., and Fuchs, E. (2009). Epidermal homeostasis: a balancing act of stem cells in the skin. Nat. Rev. Mol. Cell Biol. *10*, 207–217.

Blanpain, C., Lowry, W.E., Geoghegan, A., Polak, L., and Fuchs, E. (2004). Self-renewal, multipotency, and the existence of two cell populations within an epithelial stem cell niche. Cell *118*, 635–648.

Cai, C., Wang, H., He, H.H., Chen, S., He, L., Ma, F., Mucci, L., Wang, Q., Fiore, C., Sowalsky, A.G., et al. (2013). ERG induces androgen receptor-mediated regulation of SOX9 in prostate cancer. J. Clin. Invest. *123*, 1109–1122.

Camaj, P., Jäckel, C., Krebs, S., De Toni, E.N., Blum, H., Jauch, K.W., Nelson, P.J., and Bruns, C.J. (2014). Hypoxia-independent gene expression mediated by SOX9 promotes aggressive pancreatic tumor biology. Mol. Cancer Res. *12*, 421–432.

Candi, E., Schmidt, R., and Melino, G. (2005). The cornified envelope: a model of cell death in the skin. Nat. Rev. Mol. Cell Biol. *6*, 328–340.

Chen, T., Heller, E., Beronja, S., Oshimori, N., Stokes, N., and Fuchs, E. (2012). An RNA interference screen uncovers a new molecule in stem cell self-renewal and long-term regeneration. Nature *485*, 104–108.

Clayton, E., Doupé, D.P., Klein, A.M., Winton, D.J., Simons, B.D., and Jones, P.H. (2007). A single type of progenitor cell maintains normal epidermis. Nature *446*, 185–189.

Dai, J., Brooks, Y., Lefort, K., Getsios, S., and Dotto, G.P. (2013). The retinoid-related orphan receptor RORα promotes keratinocyte differentiation via FOXN1. PLoS ONE *8*, e70392.

Epstein, E.H. (2008). Basal cell carcinomas: attack of the hedgehog. Nat. Rev. Cancer *8*, 743–754.

Faus, I., Hsu, H.J., and Fuchs, E. (1994). Oct-6: a regulator of keratinocyte gene expression in stratified squamous epithelia. Mol. Cell. Biol. *14*, 3263–3275.

Fessing, M.Y., Mardaryev, A.N., Gdula, M.R., Sharov, A.A., Sharova, T.Y., Rapisarda, V., Gordon, K.B., Smorodchenko, A.D., Poterlowicz, K., Ferone, G., et al. (2011). p63 regulates Satb1 to control tissue-specific chromatin remodeling during development of the epidermis. J. Cell Biol. *194*, 825–839.

Fortunel, N.O., Otu, H.H., Ng, H.H., Chen, J., Mu, X., Chevassut, T., Li, X., Joseph, M., Bailey, C., Hatzfeld, J.A., et al. (2003). Comment on "'Stemness': transcriptional profiling of embryonic and adult stem cells" and "A stem cell molecular signature". Science *302*, 393.

Goicoechea, S.M., Arneman, D., and Otey, C.A. (2008). The role of palladin in actin organization and cell motility. Eur. J. Cell Biol. *87*, 517–525.

Grachtchouk, M., Pero, J., Yang, S.H., Ermilov, A.N., Michael, L.E., Wang, A., Wilbert, D., Patel, R.M., Ferris, J., Diener, J., et al. (2011). Basal cell carcinomas in mice arise from hair follicle stem cells and multiple epithelial progenitor populations. J. Clin. Invest. *121*, 1768–1781.

Horsley, V., Aliprantis, A.O., Polak, L., Glimcher, L.H., and Fuchs, E. (2008). NFATc1 balances quiescence and proliferation of skin stem cells. Cell *132*, 299–310.

Jensen, K.B., and Watt, F.M. (2006). Single-cell expression profiling of human epidermal stem and transit-amplifying cells: Lrig1 is a regulator of stem cell quiescence. Proc. Natl. Acad. Sci. USA *103*, 11958–11963.

Jones, P.H., and Watt, F.M. (1993). Separation of human epidermal stem cells from transit amplifying cells on the basis of differences in integrin function and expression. Cell *73*, 713–724.

Kadaja, M., Keyes, B.E., Lin, M., Pasolli, H.A., Genander, M., Polak, L., Stokes, N., Zheng, D., and Fuchs, E. (2014). SOX9: a stem cell transcriptional regulator of secreted niche signaling factors. Genes Dev. *28*, 328–341.

Kasper, M., Jaks, V., Are, A., Bergström, Å., Schwäger, A., Svärd, J., Teglund, S., Barker, N., and Toftgård, R. (2011). Wounding enhances epidermal tumorigenesis by recruiting hair follicle keratinocytes. Proc. Natl. Acad. Sci. USA *108*, 4099–4104.

Kopp, J.L., von Figura, G., Mayes, E., Liu, F.F., Dubois, C.L., Morris, J.P., 4th, Pan, F.C., Akiyama, H., Wright, C.V., Jensen, K., et al. (2012). Identification of Sox9-dependent acinar-to-ductal reprogramming as the principal mechanism for initiation of pancreatic ductal adenocarcinoma. Cancer Cell *22*, 737–750.

Lechler, T., and Fuchs, E. (2005). Asymmetric cell divisions promote stratification and differentiation of mammalian skin. Nature *437*, 275–280.

Lefebvre, V., Huang, W., Harley, V.R., Goodfellow, P.N., and de Crombrugghe, B. (1997). SOX9 is a potent activator of the chondrocyte-specific enhancer of the pro alpha1(II) collagen gene. Mol. Cell. Biol. *17*, 2336–2346.

Liu, J., Pan, S., Hsieh, M.H., Ng, N., Sun, F., Wang, T., Kasibhatla, S., Schuller, A.G., Li, A.G., Cheng, D., et al. (2013). Targeting Wnt-driven cancer through the inhibition of Porcupine by LGK974. Proc. Natl. Acad. Sci. USA *110*, 20224–20229.

Mascré, G., Dekoninck, S., Drogat, B., Youssef, K.K., Broheé, S., Sotiropoulou, P.A., Simons, B.D., and Blanpain, C. (2012). Distinct contribution of stem and progenitor cells to epidermal maintenance. Nature *489*, 257–262.

Moser, M., Binder, O., Wu, Y., Aitsebaomo, J., Ren, R., Bode, C., Bautch, V.L., Conlon, F.L., and Patterson, C. (2003). BMPER, a novel endothelial cell precursor-derived protein, antagonizes bone morphogenetic protein signaling and endothelial cell differentiation. Mol. Cell. Biol. *23*, 5664–5679.

Najm, P., and El-Sibai, M. (2014). Palladin regulation of the actin structures needed for cancer invasion. Cell Adhes. Migr. *8*, 29–35.

Nguyen, H., Merrill, B.J., Polak, L., Nikolova, M., Rendl, M., Shaver, T.M., Pasolli, H.A., and Fuchs, E. (2009). Tcf3 and Tcf4 are essential for long-term homeostasis of skin epithelia. Nat. Genet. *41*, 1068–1075.

Nishino, J., Kim, I., Chada, K., and Morrison, S.J. (2008). Hmga2 promotes neural stem cell self-renewal in young but not old mice by reducing p16Ink4a and p19Arf Expression. Cell *135*, 227–239.

Nowak, J.A., Polak, L., Pasolli, H.A., and Fuchs, E. (2008). Hair follicle stem cells are specified and function in early skin morphogenesis. Cell Stem Cell *3*, 33–43.

Palmer, C.J., Galan-Caridad, J.M., Weisberg, S.P., Lei, L., Esquilin, J.M., Croft, G.F., Wainwright, B., Canoll, P., Owens, D.M., and Reizis, B. (2014). Zfx facilitates tumorigenesis caused by activation of the Hedgehog pathway. Cancer Res. *74*, 5914–5924.

Rhee, H., Polak, L., and Fuchs, E. (2006). Lhx2 maintains stem cell character in hair follicles. Science *312*, 1946–1949.

Shi, G., Sohn, K.C., Li, Z., Choi, D.K., Park, Y.M., Kim, J.H., Fan, Y.M., Nam, Y.H., Kim, S., Im, M., et al. (2013). Expression and functional role of Sox9 in human epidermal keratinocytes. PLoS ONE *8*, e54355.

Stratton, M.R. (2011). Exploring the genomes of cancer cells: progress and promise. Science *331*, 1553–1558.

Thomsen, M.K., Ambroisine, L., Wynn, S., Cheah, K.S., Foster, C.S., Fisher, G., Berney, D.M., Møller, H., Reuter, V.E., Scardino, P., et al.; Transatlantic Prostate Group (2010). SOX9 elevation in the prostate promotes proliferation and cooperates with PTEN loss to drive tumor formation. Cancer Res. *70*, 979–987.

Vidal, V.P., Chaboissier, M.C., Lutzkendorf, S., Cotsarelis, G., Mill, P., Hui, C.C., Ortonne, N., Ortonne, J.P., and Schedl, A. (2005). Sox9 is essential for outer root sheath differentiation and the formation of the hair stem cell compartment. Curr. Biol. *15*, 1340–1351.

Vidal, V.P., Ortonne, N., and Schedl, A. (2008). SOX9 expression is a general marker of basal cell carcinoma and adnexal-related neoplasms. J. Cutan. Pathol. *35*, 373–379.

Wang, H., Leav, I., Ibaragi, S., Wegner, M., Hu, G.F., Lu, M.L., Balk, S.P., and Yuan, X. (2008). SOX9 is expressed in human fetal prostate epithelium and enhances prostate cancer invasion. Cancer Res. *68*, 1625–1630.

Wang, G.Y., Wang, J., Mancianti, M.L., and Epstein, E.H., Jr. (2011). Basal cell carcinomas arise from hair follicle stem cells in Ptch1(+/-) mice. Cancer Cell *19*, 114–124.

Witke, W., Sharpe, A.H., Hartwig, J.H., Azuma, T., Stossel, T.P., and Kwiatkowski, D.J. (1995). Hemostatic, inflammatory, and fibroblast responses are blunted in mice lacking gelsolin. Cell *81*, 41–51.

Wong, S.Y., and Reiter, J.F. (2011). Wounding mobilizes hair follicle stem cells to form tumors. Proc. Natl. Acad. Sci. USA *108*, 4093–4098.

Wu, X., Shen, Q.T., Oristian, D.S., Lu, C.P., Zheng, Q., Wang, H.W., and Fuchs, E. (2011). Skin stem cells orchestrate directional migration by regulating microtubule-ACF7 connections through GSK3β. Cell *144*, 341–352.

Yang, S.H., Andl, T., Grachtchouk, V., Wang, A., Liu, J., Syu, L.J., Ferris, J., Wang, T.S., Glick, A.B., Millar, S.E., and Dlugosz, A.A. (2008). Pathological responses to oncogenic Hedgehog signaling in skin are dependent on canonical Wnt/beta3-catenin signaling. Nat. Genet. *40*, 1130–1135.

Youssef, K.K., Van Keymeulen, A., Lapouge, G., Beck, B., Michaux, C., Achouri, Y., Sotiropoulou, P.A., and Blanpain, C. (2010). Identification of the cell lineage at the origin of basal cell carcinoma. Nat. Cell Biol. *12*, 299–305.

Youssef, K.K., Lapouge, G., Bouvrée, K., Rorive, S., Brohée, S., Appelstein, O., Larsimont, J.C., Sukumaran, V., Van de Sande, B., Pucci, D., et al. (2012). Adult interfollicular tumour-initiating cells are reprogrammed into an embryonic hair follicle progenitor-like fate during basal cell carcinoma initiation. Nat. Cell Biol. *14*, 1282–1294.